Variational optimization of the second order density matrix derived from a seniority-zero configuration interaction wave function

Ward Poelmans,[*,†] Mario Van Raemdonck,[‡] Brecht Verstichel,[†] Stijn De Baerdemacker,[†,‡] Alicia Torre,[¶] Luis Lain,[¶] Gustavo E. Massaccesi,[§] Diego R. Alcoba,[‖] Patrick Bultinck,[‡] and Dimitri Van Neck[†]

[†]*Center for Molecular Modeling, Ghent University, Technologiepark 903, 9052 Zwijnaarde, Belgium*

[‡]*Department of Inorganic and Physical Chemistry, Ghent University, Krijgslaan 281 (S3), 9000 Gent, Belgium*

[¶]*Departamento de Química Física, Facultad de Ciencia y Tecnología, Universidad del País Vasco, Apdo. 644, E-48080 Bilbao, Spain*

[§]*Departamento de Ciencias Exactas, Ciclo Básico Común, Universidad de Buenos Aires, Ciudad Universitaria, 1428 Buenos Aires, Argentina*

[‖]*Departamento de Física, Facultad de Ciencias Exactas y Naturales, Universidad de Buenos Aires and Instituto de Física de Buenos Aires, Consejo Nacional de Investigaciones Científicas y Técnicas, Ciudad Universitaria, 1428 Buenos Aires, Argentina*

E-mail: wpoely86@gmail.com

Abstract

We perform a direct variational determination of the second-order (two-particle) density matrix corresponding to a many-electron system, under a restricted set of the

two-index N-representability $\mathcal{P}$-, $\mathcal{Q}$-, and $\mathcal{G}$-conditions. In addition, we impose a set of necessary constraints that the two-particle density matrix must be derivable from a doubly-occupied many-electron wave function, i.e. a singlet wave function for which the Slater determinant decomposition only contains determinants in which spatial orbitals are doubly occupied. We rederive the two-index N-representability conditions first found by Weinhold and Wilson and apply them to various benchmark systems (linear hydrogen chains, He, N_2 and CN^-). This work is motivated by the fact that a doubly-occupied many-electron wave function captures in many cases the bulk of the static correlation. Compared to the general case, the structure of doubly-occupied two-particle density matrices causes the associate semidefinite program to have a very favorable scaling as L^3, where L is the number of spatial orbitals. Since the doubly-occupied Hilbert space depends on the choice of the orbitals, variational calculation steps of the two-particle density matrix are interspersed with orbital-optimization steps (based on Jacobi rotations in the space of the spatial orbitals). We also point to the importance of symmetry breaking of the orbitals when performing calculations in a doubly-occupied framework.

1 Introduction

The main problem in many-body quantum mechanics, which comprises nuclear physics, quantum chemistry and condensed matter physics, is the exponential increase of the dimension of the Hilbert space with the number of particles. Within a given single-particle basis, a complete diagonalization in many-electron space, Full Configuration Interaction (FullCI), will provide the exact answer, but is prohibitively expensive except for small systems[1]. The challenge has therefore been to develop approximate methods capturing the relevant degrees of freedom in the system without an excessive computational cost, i.e., with a polynomial increase.

Many approximate methods have been developed over the years[1,2]. A standard approach

is to start from a mean-field (Hartree-Fock) solution and improve on this by adding excitations of increasing complexity (Coupled Cluster Theory[3,4], Perturbation Theory[4], etc.). These single-reference methods only work well when the wave function is dominated by a single Slater determinant. In bond-breaking processes, e.g., the Hartree-Fock (HF) approximation is qualitatively wrong and a multi-reference approximation is needed[5]. In Multi-configuration Self-Consistent Field (MCSCF)[1,6], one expands the wave function as a linear combination of Slater determinants (configurations), and the Configuration Interaction (CI) coefficients and the orbitals building the Slater determinants are optimized together. In the last decennia, new methods for strongly correlated systems were developed. Density Matrix Renormalization Group (DMRG)[7–10] is FullCI accurate while extending the limits far beyond what is possible with classical FullCI. Project symmetry-broken Hartree-Fock[11–13] is a mean-field scaling method in which all symmetries are broken. While it is difficult to recover symmetries once they are lost, a self-consistent variation-after-projection technique can overcome these issues[14].

Also Doubly-Occupied Configuration Interaction (DOCI)[15] received renewed interest[16–20]. In DOCI, all spatial orbitals are doubly occupied by two (spin-up/down) electrons. This is also called a seniority-zero wave function. The seniority number is the number of unpaired electrons[15,21,22]. FullDOCI is an exact diagonalization of the Hamiltonian as is FullCI, but in the Hilbert space restricted to Slater determinants where every spatial orbital is doubly occupied or empty. However, FullDOCI still suffers from factorial scaling. The interest in DOCI is motivated by its ability to describe the static correlation[15,23]. It was also realized that DOCI is the lowest rung on the ladder in a seniority hierarchy leading to FullCI[24,25]: If one adds configurations of higher seniority (2, 4, ...) in the wave function expansion, one will eventually reach the FullCI limit[15,25]. Furthermore, it can also be shown that General Valence Bond with perfect pairing is a special case of DOCI[19]. An efficient and low-scaling approximation to DOCI is available: antisymmetric product of 1-reference-orbital geminals[16,18,19] or pair-Coupled Cluster Doubles[17,20] (they are equivalent). However, like

any truncated CI wave function, DOCI is orbital dependent[15,23,24] and those approximations need an orbital optimizer. This severely deteriorates the scaling.

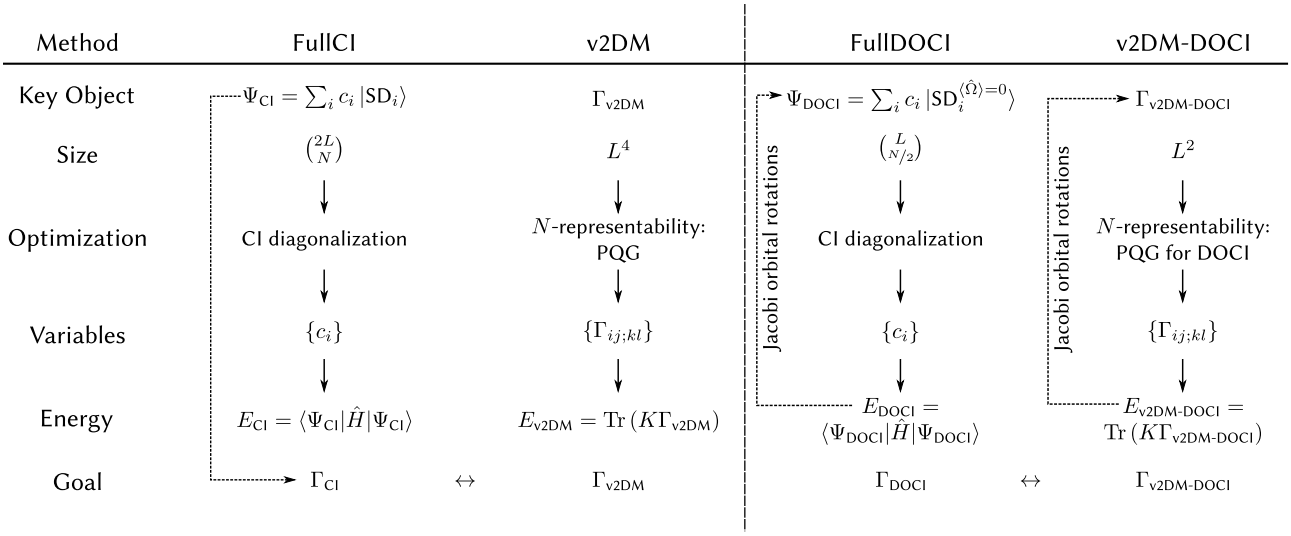

Figure 1: Overview of the methods used in this paper. $\hat{\Omega}$ is the seniority-number operator.

In the present paper, we focus on an alternative way to approximate the ground state of an N-electron system, where we dispense with the wave function altogether and concentrate on the two-particle density matrix (2DM)[26,27]. The 2DM contains the relevant information, such as all expectation values of two-particle operators, but its dimension only scales as L^4, with L the dimension of spatial orbital space. Unlike Density (Matrix) functional theory, the energy can be expressed as an exact yet simple linear function of the 2DM and a variational optimization can be used to find the ground-state energy (v2DM)[28] where the optimization should be constrained to the class of 2DM's[29,30] that can be derived from an antisymmetric wave function, the so-called N-representable 2DM's. The wave function is not used in this method and we directly start from a 2DM. Although, the burden is shifted to the characterization of the N-representable class of 2DM's. Since the complete characterization is known to be a QMA complete problem[31], one has to use a set of necessary but not (in general) sufficient conditions on the 2DM. The role of the necessary N-representability conditions is to enforce that the resulting 2DM approximates a wave function derivable 2DM as best as possible. Since the minimization of the energy is carried out over a too large set,

one obtains lower bounds to the exact energy[30].

The most commonly used conditions are derived from positive semidefinite Hamiltonians and express the fact that their expectation value in any wave function should be positive. Examples are the standard $\mathcal{P}$, $\mathcal{Q}$ and $\mathcal{G}$ two-index conditions[30,32] and the $\mathcal{T}_1$ and $\mathcal{T}_2$ three-index conditions[33]. Other kinds of conditions exist, such as subsystem constraints[34] or active-space constraints[35]. The resulting constrained optimization problem is known as a semidefinite program (SDP). This is a well-known class of convex optimization problems[36–38] for which a large collection of solvers exists[39]. We created a SDP solver tailored to v2DM[40–48]: for the two-index conditions, basic matrix operations exhibit a scaling of $(2L)^6$ and for the three-index conditions, $(2L)^9$. Unfortunately, on the whole the v2DM approach is not competitive with e.g. CCSD methods[49,50].

In this paper, we aim to study the 2DM variational optimization restricted to DOCI space, henceforth called v2DM-DOCI. In Figure 1, we give an overview of all the relevant methods. We impose necessary conditions that the wave function from which the 2DM was derived has the form of a DOCI wave function. This greatly simplifies the structure of the 2DM[51,52] which in turn leads to a much better scaling. We needs an orbital optimization scheme, which is far from trivial as the energy landscape contains a large number of local minima, many very close to or even degenerate with the ground-state energy[24]. The same problem is also encountered in MCSCF[53,54] and Valence bond Self-Consistent Field[55] where several solutions are at hand[53,56,57]. Most algorithms use the 2DM which still has to be calculated in wave function-based methods while we have it directly, although it is not totally N-representable. If a good starting point in the orbital space is available, a simple local minimizer can generate good results. In this paper we use an algorithm utilizing Jacobi rotations[58] to avoid the full simultaneous four-index transformation of the two-electron integrals.

In section 2, we introduce the v2DM framework and apply it to the case of a DOCI wave function, leading to v2DM-DOCI. In section 3 the orbital optimization scheme is presented in detail, and in section 4 results are shown for several illustrative test cases, including situations

where a multi-reference description is needed. A summary and discussion is presented in section 5.

2 Variational 2DM

We use Greek letters $\alpha, \beta, \ldots$ to denote a general spinorbital ($2L$ in total), and Roman letters $a, b, \ldots$ to denote the spatial part of the orbital (L in total). With the bar symbol, the pairing partner of a state is denoted: a and $\bar{a}$ form a pair of the same spatial orbital with opposite spin, e.g. $a = a\uparrow$ and $\bar{a} = a\downarrow$. All summations runs over either the spinorbitals or the orbitals depending on whether Greek or Roman summation indices were used. We use the second-quantization formalism: $\hat{a}^\dagger_\alpha$ ($\hat{a}_\alpha$) denotes a creation (annihilation) operator for a fermion in the single particle state α. It is also assumed that the many-electron wave function is real.

2.1 General v2DM

In second quantization a Hamiltonian with pairwise interactions can be written as[59]

$$\hat{H} = \sum_{\alpha\beta} \langle\alpha|\hat{T}|\beta\rangle\, \hat{a}^\dagger_\alpha \hat{a}_\beta + \frac{1}{4} \sum_{\alpha\beta\gamma\delta} \langle\alpha\beta|\hat{V}|\gamma\delta\rangle\, \hat{a}^\dagger_\alpha \hat{a}^\dagger_\beta \hat{a}_\delta \hat{a}_\gamma \ , \tag{1}$$

where $\hat{T}$ and $\hat{V}$ are the one- and two-particle operators. It should be noted that the formalism is completely general for Hamiltonians up to two-body interactions, however all operators discussed in the present paper concern field-free, non-relativistic electronic structure Hamiltonians, i.e. $\hat{T}$ is the sum of the electronic kinetic energy and the nuclei-electron attraction, whereas $\hat{V}$ represents the interelectronic Coulomb repulsion. The ground-state energy can be expressed solely in terms of the second order reduced density matrix (2DM)[26] Γ,

$$E = \mathrm{Tr}\,(K\Gamma) = \frac{1}{4} \sum_{\alpha\beta\gamma\delta} K_{\alpha\beta;\gamma\delta} \Gamma_{\alpha\beta;\gamma\delta} \ , \tag{2}$$

where

$$\Gamma_{\alpha\beta;\gamma\delta} = \langle\psi|\hat{a}^\dagger_\alpha\hat{a}^\dagger_\beta\hat{a}_\delta\hat{a}_\gamma|\psi\rangle \ , \tag{3}$$

$$K_{\alpha\beta;\gamma\delta} = \frac{1}{N-1}\left(T_{\alpha\gamma}\delta_{\beta\delta} - T_{\beta\gamma}\delta_{\alpha\delta} - T_{\alpha\delta}\delta_{\beta\gamma} + T_{\beta\delta}\delta_{\alpha\gamma}\right) + V_{\alpha\beta\gamma\delta} \ , \tag{4}$$

with $|\psi\rangle$ the ground-state wave function for the Hamiltonian (1) with matrix elements $T_{\alpha\beta} = \langle\alpha|\hat{T}|\beta\rangle$ and $V_{\alpha\beta\gamma\delta} = \langle\alpha\beta|\hat{V}|\gamma\delta\rangle$. N is the number of particles, and (3) and (4) define matrix elements of the 2DM and the reduced Hamiltonian $K_{\alpha\beta;\gamma\delta}$, respectively. Some elementary properties are easily derived,

$$\Gamma_{\alpha\beta;\gamma\delta} = -\Gamma_{\beta\alpha;\gamma\delta} = -\Gamma_{\alpha\beta;\delta\gamma} = \Gamma_{\beta\alpha;\delta\gamma} \ , \tag{5}$$

$$\Gamma_{\alpha\beta;\gamma\delta} = \Gamma_{\gamma\delta;\alpha\beta} \ , \tag{6}$$

$$\mathrm{Tr}\,(\Gamma) = \frac{1}{2}\sum_{\alpha\beta}\Gamma_{\alpha\beta;\alpha\beta} = \frac{N(N-1)}{2} \ . \tag{7}$$

The idea of variational 2DM is to minimize the energy functional (2). The 2DM is a much more compact object than the wave function as its matrix dimension scales as L^2. However, a direct approach produces unrealistic energies[28]. The variation has to be limited to the class of N-representable 2DM's[29,30]: for every 2DM, there must exist a wave function $|\psi\rangle$ such that (3) is satisfied. Unfortunately there exists no straightforward way of establishing whether a 2DM is N-representable. The necessary and sufficient conditions are formally known[60,61]: a 2DM is N-representable if and only if, for every two-particle Hamiltonian $\hat{H}_\phi$, the following inequality is true:

$$\mathrm{Tr}\,(K_\phi\Gamma) \geq E_0(\hat{H}_\phi) \ , \tag{8}$$

with K_ϕ the reduced Hamiltonian and $E_0(\hat{H}_\phi)$ the exact ground-state energy of the Hamiltonian $\hat{H}_\phi$. This theorem cannot be used as a sufficient condition for N-representability as that would require the ground-state energy of every possible two-particle Hamiltonian $\hat{H}_\phi$, but it can be used as a necessary condition: the theorem (8) can be relaxed to Hamiltonians for which a lower bound to its ground-state energy is known. A straightforward choice is

$$\hat{H} = \hat{B}^\dagger \hat{B}, \tag{9}$$

a class of manifestly positive semidefinite Hamiltonians. If we restrict $\hat{B}$ to the two-particle space, we find the well-known $\mathcal{P}$, $\mathcal{Q}$ and $\mathcal{G}$ two-index conditions:

1. The $\mathcal{P}$ condition: $\hat{B} = \sum_{\alpha\beta} p_{\alpha\beta} \hat{a}_\alpha \hat{a}_\beta$, for arbitrary $p_{\alpha\beta}$. This trivial condition imposes the positive semidefiniteness of the 2DM itself:

$$\begin{aligned} \mathcal{P}(\Gamma)_{\alpha\beta;\gamma\delta} &= \langle\psi|\hat{a}^\dagger_\alpha \hat{a}^\dagger_\beta \hat{a}_\delta \hat{a}_\gamma|\psi\rangle \\ \mathcal{P}(\Gamma) &= \Gamma \succeq 0 \end{aligned} \tag{10}$$

2. The $\mathcal{Q}$ condition[30]: $\hat{B} = \sum_{\alpha\beta} q_{\alpha\beta} \hat{a}^\dagger_\alpha \hat{a}^\dagger_\beta$, for arbitrary $q_{\alpha\beta}$ leading to

$$\mathcal{Q}(\Gamma) \succeq 0 \ , \tag{11}$$

where

$$\begin{aligned} \mathcal{Q}(\Gamma)_{\alpha\beta;\gamma\delta} &= \langle\psi|\hat{a}_\alpha \hat{a}_\beta \hat{a}^\dagger_\delta \hat{a}^\dagger_\gamma|\psi\rangle \\ &= \Gamma_{\alpha\beta;\gamma\delta} + (\delta_{\alpha\gamma}\delta_{\beta\delta} - \delta_{\beta\gamma}\delta_{\alpha\delta}) \frac{2\mathrm{Tr}\,(\Gamma)}{N(N-1)} \\ &\quad -\delta_{\alpha\gamma}\rho_{\beta\delta} + \delta_{\beta\gamma}\rho_{\alpha\delta} + \delta_{\alpha\delta}\rho_{\beta\gamma} - \delta_{\beta\delta}\rho_{\alpha\gamma} \ . \end{aligned} \tag{12}$$

and the single-particle density matrix (1DM) is defined as

$$\rho_{\alpha\beta} = \langle\psi|\hat{a}^\dagger_\alpha \hat{a}_\beta|\psi\rangle = \frac{1}{N-1}\sum_\lambda \Gamma_{\alpha\lambda;\beta\lambda} \ . \tag{13}$$

3. The $\mathcal{G}$ condition[32]: $\hat{B} = \sum_{\alpha\beta} g_{\alpha\beta}\hat{a}^\dagger_\alpha \hat{a}_\beta$, for arbitrary $g_{\alpha\beta}$,

$$\mathcal{G}(\Gamma) \succeq 0 \tag{14}$$

with

$$\mathcal{G}(\Gamma)_{\alpha\beta;\gamma\delta} = \langle\psi|\hat{a}^\dagger_\alpha \hat{a}_\beta \hat{a}^\dagger_\delta \hat{a}_\gamma|\psi\rangle = \delta_{\beta\delta}\rho_{\alpha\gamma} - \Gamma_{\alpha\delta;\gamma\beta} \ . \tag{15}$$

Furthermore, there are the so-called three-index commutator conditions[33,48,62–65] which are computationally much more demanding and are not used in this paper. All these conditions are necessary but not sufficient: the true N-representable space is much more restricted. Because of this, v2DM will always find a lower bound to the FullCI energy.

The variational optimization of the 2DM can now be expressed as:

$$\begin{gathered} \min \mathrm{Tr}\,(K\Gamma) \quad \text{while} \\ \mathcal{P}(\Gamma) \oplus \mathcal{Q}(\Gamma) \oplus \mathcal{G}(\Gamma) \succeq 0 \\ \mathrm{Tr}\,(\Gamma) = \frac{N(N-1)}{2} \ . \end{gathered} \tag{16}$$

This optimization problem can be formulated as a semidefinite program (SDP)[46,47], a class of well-known convex optimization problems[36] for which general-purpose solvers exists[39,66,67]. Earlier we developed SDP solvers customized for v2DM that exploit the specific structure of the problem[40,43,44,68]. Such solvers are much more efficient than the general-purpose solvers. In this paper we use a boundary point method[41,69,70] to solve the SDP problem. In this method, the primal-dual gap is zero by definition, and convergence is reached when both primal and dual feasibility is achieved. The computationally most intensive step in this

algorithm is the calculation of the eigenvalues and eigenvectors of the constraint matrices. The computational cost of the program scales as L^6 for floating-point operations and L^4 for memory when using the two-index conditions. A detailed explanation of the solvers can be found in Ref 68.

2.2 DOCI tailored v2DM

We now impose the additional condition that $|\psi\rangle$ in (3) is a DOCI wave function. In principle any pairing scheme can be used, but the natural choice is the singlet pairing scheme, in which each spatial orbital is occupied by two electrons of opposite spin. This is based on the assumption that the most important static correlations in a closed-shell molecule can be captured in this way[15]. In CI terms, the wave function can be expanded in Slater determinants where all spatial orbitals are doubly occupied. This is also called a seniority-zero wave function. Formally, the DOCI wave function can be written as

$$|\psi\rangle = \sum_{a_1 \ldots a_{(N/2)}} c_{a_1 \ldots a_{(N/2)}} \prod_{k=1}^{N/2} \hat{a}^\dagger_{a_k} \hat{a}^\dagger_{\bar{a}_k} |\rangle \ , \tag{17}$$

where the $a_i = 1 \ldots L$ summations are over all spatial orbitals (L) and $|\rangle$ is defined as the particle vacuum.

A simple approach would be to project the reduced Hamiltonian (4) onto DOCI space and use existing v2DM codes. However, this does not lead to the desired result as internal consistency conditions on the 2DM are needed (see below). Also, any computational advantages due to the DOCI structure are lost as the scaling of the program remains unaltered.

It is much more efficient to adapt the N-representability conditions to the DOCI case as they are drastically simplified. The adapted DOCI conditions were already derived by Weinhold and Wilson[51,52] but to the best of our knowledge never exploited in practical calculations.

Since we work in DOCI space, all operators evaluated between two DOCI wave functions

need to have seniority-zero, *i.e.* they cannot change the number of broken pairs. This immediately implies that the 1DM is diagonal and that the chosen set of orbitals is also the set of natural orbitals of $|\psi\rangle$:

$$\begin{aligned} \rho_{ab} &= \langle\psi|\hat{a}_a^\dagger \hat{a}_b|\psi\rangle = \langle\psi|\hat{a}_{\bar{a}}^\dagger \hat{a}_{\bar{b}}|\psi\rangle = \delta_{ab}\rho_a \ , \\ & \langle\psi|\hat{a}_a^\dagger \hat{a}_{\bar{b}}|\psi\rangle = \langle\psi|\hat{a}_{\bar{a}}^\dagger \hat{a}_b|\psi\rangle = 0 \ . \end{aligned} \tag{18}$$

Furthermore, it is clear that

$$\rho_a \geq 0 \ , \tag{19}$$

$$\sum_a \rho_a = \frac{N}{2} \ . \tag{20}$$

A similar simplification occurs for the 2DM and the $\mathcal{PQG}$ conditions:

1. The $\mathcal{P}$ condition. The operator $\hat{B}$ in eq. (9) acting on a DOCI wave functions can create both a seniority-0 and seniority-2 state. The corresponding $\hat{B}^\dagger$ operator can only connect states of the same seniority and therefore block diagonalization will occur. The seniority-0 block is the pair density matrix,

$$\forall a, b: \quad \langle\psi|\hat{a}_a^\dagger \hat{a}_{\bar{a}}^\dagger \hat{a}_{\bar{b}} \hat{a}_b|\psi\rangle = \Gamma_{a\bar{a};b\bar{b}} = \Pi_{ab} \ . \tag{21}$$

From the positivity of the Hamiltonian $\hat{B}^\dagger \hat{B}$ with

$$\hat{B}^\dagger = \sum_a p_a \hat{a}_a^\dagger \hat{a}_{\bar{a}}^\dagger \ , \tag{22}$$

it follows that the $L \times L$ pair density matrix has to be positive semidefinite,

$$\Pi \succeq 0 \ . \tag{23}$$

The seniority-2 block is a part of the diagonal of the 2DM:

$$\begin{aligned} \forall a \neq b: \quad \langle\psi|\hat{a}_a^\dagger \hat{a}_b^\dagger \hat{a}_b \hat{a}_a|\psi\rangle &= \langle\psi|\hat{a}_{\bar{a}}^\dagger \hat{a}_b^\dagger \hat{a}_b \hat{a}_{\bar{a}}|\psi\rangle = \\ \langle\psi|\hat{a}_a^\dagger \hat{a}_{\bar{b}}^\dagger \hat{a}_{\bar{b}} \hat{a}_a|\psi\rangle &= \langle\psi|\hat{a}_{\bar{a}}^\dagger \hat{a}_{\bar{b}}^\dagger \hat{a}_{\bar{b}} \hat{a}_{\bar{a}}|\psi\rangle = \\ \Gamma_{ab;ab} &= D_{ab} \geq 0 \end{aligned} \tag{24}$$

For convenience we put $D_{aa} = 0$. Equation (24) provides $\frac{L(L-1)}{2}$ linear inequalities that have to be imposed. There are now two independent ways of obtaining the 1DM out of the 2DM: via the trace relation (13) and via the diagonal part of the pairing matrix:

$$\rho_a = \frac{2}{N-2} \sum_b D_{ab} \ , \tag{25}$$

$$\rho_a = \Pi_{aa} \ , \tag{26}$$

as the operators $\hat{a}_a^\dagger \hat{a}_a = \hat{a}_{\bar{a}}^\dagger \hat{a}_{\bar{a}} = \hat{a}_a^\dagger \hat{a}_{\bar{a}}^\dagger \hat{a}_{\bar{a}} \hat{a}_a$ have the same expectation value for a DOCI wave function. These consistency conditions have to be separately enforced. Note that the trace condition (7) can be written in two alternative ways:

$$\sum_a \Pi_{aa} = \frac{N}{2}, \quad \text{and} \quad \sum_{ab} D_{ab} = \frac{N}{4}(N-2) \ . \tag{27}$$

2. The $\mathcal{Q}$ condition has exactly the same structure as the $\mathcal{P}$ condition. The constraint for the seniority-0 block is derived from

$$\sum_{ab} q_a \, \langle\psi|\hat{a}_a \hat{a}_{\bar{a}} \hat{a}_{\bar{b}}^\dagger \hat{a}_b^\dagger|\psi\rangle \, q_b \geq 0 \ , \tag{28}$$

which leads to the positivity condition $\mathcal{Q}^\Pi \succeq 0$ on a $L \times L$ matrix $\mathcal{Q}^\Pi$, with elements

$$\mathcal{Q}^\Pi_{ab} = \delta_{ab}(1 - \rho_a - \rho_b) + \Pi_{ab} \ . \tag{29}$$

The seniority-2 part gives rise to a set of linear inequalities,

$$\forall a \neq b: \quad \langle\psi|\hat{a}_a\hat{a}_b\hat{a}_b^\dagger\hat{a}_a^\dagger|\psi\rangle = 1 - \rho_a - \rho_b + D_{ab} \geq 0 \ . \tag{30}$$

3. The $\mathcal{G}$ condition is somewhat more complex as more combinations are non-zero. We work systematically according to seniority and spin.

   Spin projections $M_S = \pm 1$ are equivalent, so we only consider the $M_S = +1$ case and always assume $a \neq b$, since in DOCI space $\hat{a}_a^\dagger\hat{a}_{\bar{a}}\,|\psi\rangle = 0$. The particle-hole operators generating this constraint are of the form $\hat{B}^\dagger = \sum_{ab} g_{ab}\hat{a}_a^\dagger\hat{a}_{\bar{b}}$ which lead to the following seniority-2 positivity condition:

$$\begin{aligned}\sum_{abcd} g_{ab}\left[\delta_{bd}\delta_{ac}(\rho_a - D_{ab}) - \delta_{ad}\delta_{bc}\Pi_{ab}\right] g_{cd} = \\ \sum_{ab} g_{ab}\left[(\rho_a - D_{ab})g_{ab} - \Pi_{ab}g_{ba}\right] \geq 0\end{aligned} \tag{31}$$

   This condition is almost diagonal, as g_{ab} is only connected with itself and g_{ba}, leading to the following 2×2 positivity condition:

$$\forall a < b \qquad \begin{bmatrix} \rho_a - D_{ab} & -\Pi_{ab} \\ -\Pi_{ab} & \rho_b - D_{ab} \end{bmatrix} \succeq 0 \ . \tag{32}$$

   For the $M_S = 0$ and seniority-2 case, the particle-hole operators are of the form $\hat{B}_1^\dagger = \sum_{ab} g_{ab}\hat{a}_a^\dagger\hat{a}_b$ and $\hat{B}_2^\dagger = \sum_{ab} g_{ab}\hat{a}_{\bar{a}}^\dagger\hat{a}_{\bar{b}}$, with $a \neq b$. These terms are coupled to each other. The diagonal terms ($\hat{B}_1^\dagger\hat{B}_1$ and $\hat{B}_2^\dagger\hat{B}_2$) are

$$\langle\psi|\hat{a}_a^\dagger\hat{a}_b\hat{a}_d^\dagger\hat{a}_c|\psi\rangle = \delta_{ac}\delta_{bd}(\rho_a - D_{ab}) \ . \tag{33}$$

The off-diagonal terms ($\hat{B}_1^\dagger \hat{B}_2$ and $\hat{B}_2^\dagger \hat{B}_1$) are

$$\langle\psi|\hat{a}_a^\dagger \hat{a}_b \hat{a}_{\bar{d}}^\dagger \hat{a}_{\bar{c}}|\psi\rangle = \delta_{ad}\delta_{bc}\Pi_{ab} \ , \tag{34}$$

which leads to the 2×2 constraint matrix

$$\forall a < b \qquad \begin{bmatrix} \rho_a - D_{ab} & \Pi_{ab} \\ \Pi_{ab} & \rho_b - D_{ab} \end{bmatrix} \succeq 0 \ , \tag{35}$$

which is equivalent to (32).

The $M_S = 0$ and seniority-0 part is built by two particle-hole operators $\hat{B}_1^\dagger = \sum_a g_a \hat{a}_a^\dagger \hat{a}_a$ and $\hat{B}_2^\dagger = \sum_b g_b \hat{a}_{\bar{b}}^\dagger \hat{a}_{\bar{b}}$. This leads to a $2L \times 2L$ matrix with diagonal elements ($\hat{B}_1^\dagger \hat{B}_1$ and $\hat{B}_2^\dagger \hat{B}_2$)

$$\langle\psi|\hat{a}_a^\dagger \hat{a}_a \hat{a}_b^\dagger \hat{a}_b|\psi\rangle = \delta_{ab}\rho_a + D_{ab} \ , \tag{36}$$

and off-diagonal elements ($\hat{B}_1^\dagger \hat{B}_2$ and $\hat{B}_2^\dagger \hat{B}_1$)

$$\begin{aligned} \langle\psi|\hat{a}_a^\dagger \hat{a}_a \hat{a}_{\bar{b}}^\dagger \hat{a}_{\bar{b}}|\psi\rangle &= D_{ab} + \delta_{ab}\Pi_{ab} \\ &= \delta_{ab}\rho_a + D_{ab} \ . \end{aligned} \tag{37}$$

Both blocks are identical, which means that L eigenvalues will be zero and we only have to impose the positivity $\mathcal{G}^\Pi \succeq 0$ of a $L \times L$ matrix:

$$\mathcal{G}_{ab}^\Pi = \delta_{ab}\rho_a + D_{ab} \ . \tag{38}$$

The $\mathcal{P}$ conditions correspond to eq. (24a) and (30) in Weinhold and Wilson [52], the $\mathcal{Q}$ conditions to eq. (24b) and (34) and the $\mathcal{G}$ conditions to eq. (24c), (44) and (18).

We now look at the reduced Hamiltonian (4) which simplifies to the same structure as

the $\mathcal{P}$ condition. The DOCI reduced Hamiltonian is

$$\begin{aligned} K^{\Pi}_{ab} &= \frac{2}{N-1} T_{aa}\delta_{ab} + V_{aabb} \ , \\ K^{D}_{ab} &= \frac{1}{N-1}\left(T_{aa} + T_{bb}\right) + V_{abab} - \frac{1}{2} V_{abba} \ . \end{aligned} \tag{39}$$

The energy functional (2) for DOCI becomes

$$E = \sum_{ab} \left(K^{\Pi}_{ab}\Pi_{ab} + 2K^{D}_{ab}D_{ab} \right) \ . \tag{40}$$

An advantage of v2DM-DOCI is that the resulting 2DM belongs to a singlet state, while the general v2DM needs additional constraints to ensure the singlet:

$$\langle\psi|\hat{a}^{\dagger}_{\alpha}\hat{a}_{\beta}\hat{S}_z|\psi\rangle = 0 \ , \tag{41}$$

with the $\hat{S}_z$ operator defined as,

$$\hat{S}_z = \frac{1}{2}\sum_{a}\left(\hat{a}^{\dagger}_{a}\hat{a}_{a} - \hat{a}^{\dagger}_{\bar{a}}\hat{a}_{\bar{a}}\right) \ . \tag{42}$$

In full v2DM, this constraint needs to be enforced by a zero eigenvalue in the $\mathcal{G}$ matrix[49,68]. In v2DM-DOCI however,

$$\begin{aligned} &\langle\psi|\hat{a}^{\dagger}_{c}\hat{a}_{d}\hat{S}_z|\psi\rangle = \\ &= \frac{1}{2}\delta_{cd}\sum_{a}^{L}\left(\langle\psi|\hat{a}^{\dagger}_{c}\hat{a}_{d}\hat{a}^{\dagger}_{a}\hat{a}_{a}|\psi\rangle - \langle\psi|\hat{a}^{\dagger}_{c}\hat{a}_{d}\hat{a}^{\dagger}_{\bar{a}}\hat{a}_{\bar{a}}|\psi\rangle\right) \\ &= \frac{1}{2}\sum_{a}^{L}\left(\langle\psi|\hat{a}^{\dagger}_{a}\hat{a}_{a}|\psi\rangle - \langle\psi|\hat{a}^{\dagger}_{c}\hat{a}^{\dagger}_{a}\hat{a}_{c}\hat{a}_{a}|\psi\rangle - \langle\psi|\hat{a}^{\dagger}_{c}\hat{a}^{\dagger}_{\bar{a}}\hat{a}_{c}\hat{a}_{\bar{a}}|\psi\rangle\right) \\ &= \frac{1}{2}\sum_{a}^{L}\left(\rho_a + (1-\delta_{ac})D_{ac} - \Pi_{ac}\delta_{ac} - (1-\delta_{ac})D_{ca}\right) \\ &= 0 \ , \end{aligned}$$

which means that the singlet condition is automatically fulfilled. It must be noted that (41) is a necessary but not sufficient condition for the 2DM to be derivable from a $S = 0$ wave function.

In these DOCI N-representability conditions, the largest matrix dimension encountered is L as compared to $(2L)^2$ in the general case. The remainder of the conditions are linear inequalities and the positive semidefiniteness of 2×2 matrices which are trivial to impose. The scaling of our code has been reduced from L^6 to L^3 for the floating point operations and from L^4 to L^2 for the memory. In Figure 2 the scaling of the v2DM and v2DM-DOCI (without orbital optimization) is shown for a growing chain of equidistant hydrogen atoms (interatomic distance = 2 Bohr) in the STO-3G basis. Note that for 30 H-atoms the v2DM-DOCI is already three orders of magnitude faster than the general v2DM code. We used a v2DM code that exploits spin symmetry and the singlet conditions are enforced, so we can make a fair comparison with v2DM-DOCI. The v2DM-DOCI starts to exhibit a smooth scaling with the number of hydrogen atoms when the runtime was at least 10^4 seconds whereas the general v2DM reaches this point sooner (10^3 seconds). We performed a linear fit on a log-log plot to find the power of the leading term in the scaling (αx^β) resulting in the coefficients found in table 1. The scaling is two orders better while the prefactor changes

Table 1: The resulting coefficients of the linear fit in Figure 2

	α	β
v2DM	$2.602\ 10^{-5}$	6.485
v2DM-DOCI	$5.268\ 10^{-5}$	3.954

little. Note that the actual scaling parameters $\beta = 6.4$ (v2DM) and $\beta = 3.9$ (v2DM-DOCI) deviate from the theoretical scaling parameters $\beta = 6$ (v2DM) and $\beta = 3$ (v2DM-DOCI) involved in the v2DM floating point operations as any v2DM algorithm contains an iterative scheme with a number of loops that slowly increases with L.

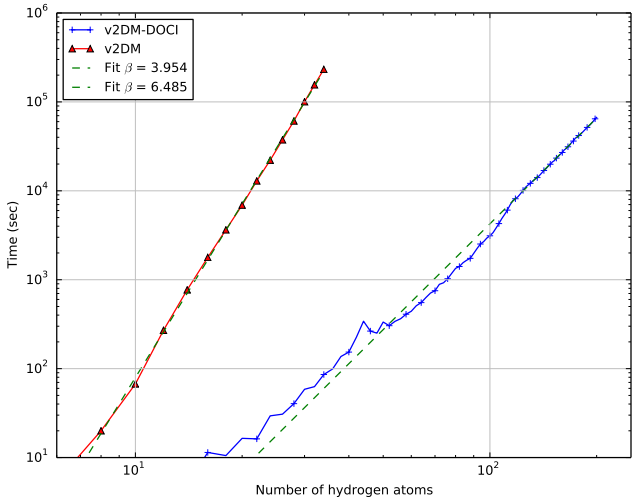

Figure 2: Scaling of v2DM-DOCI vs v2DM on a hydrogen chain (interatomic distance = 2 Bohr) in the STO-3G basis on a log-log plot. We fitted a linear curve ($\beta x + \alpha$) to the data.

3 Orbital Optimization

The DOCI energy is orbital dependent, therefore the choice of the orbitals is crucial. Like in many MCSCF methods, we use an iterative two-step algorithm[1,54,57,71–73] in which we first optimize the 2DM and then the orbitals. Orbital optimization is a hard problem as it requires finding the global minimum in a rough and uncharted landscape[24]. There are no known computationally feasible techniques for achieving this in a general way. The most often used approach is to pick a good starting point and use a Newton-Raphson based algorithm to find a local minimum[56,57]. This involves calculating the computationally expensive Jacobian and Hessian. Furthermore, the four-index transformation of the two-electron integrals is not cheap.

We use a different approach: a Jacobi rotation is performed in every step. A Jacobi rotation[58] is a unitary transformation that rotates in a two-dimensional subspace of the orbital space. While in a Newton-Raphson method all orbitals are updated at every step, in a Jacobi rotation only two orbitals are updated in each step. Jacobi rotations have the advantage of simplicity: only 2 rows and columns need to be updated, which makes the transformation of the two-electron integrals much faster. The Jacobi rotation of orbitals k

and l over an angle θ is determined by the rotation matrix

$$Q^{kl} = \begin{array}{c} \\ k \\ \\ l \\ \\ \end{array} \begin{array}{c} \begin{array}{cccccc} & & k & & l & \end{array} \\ \begin{pmatrix} 1 & & & & & \\ & \ddots & & & & \\ & & \cos\theta & \cdots & -\sin\theta & \\ & & \vdots & \ddots & \vdots & \\ & & \sin\theta & \cdots & \cos\theta & \\ & & & & & \ddots \\ & & & & & & 1 \end{pmatrix} \end{array}, \tag{43}$$

or more formally,

$$\begin{aligned} Q_{ij}^{kl} = \delta_{ij} &+ (\delta_{ik}\delta_{jk} + \delta_{il}\delta_{jl})(\cos\theta - 1) \\ &+ (\delta_{ik}\delta_{jl} - \delta_{il}\delta_{jk})\sin\theta \end{aligned} \tag{44}$$

If we apply a unitary transformation to the matrix elements (39) and insert them in the energy functional (40), we find

$$\begin{aligned} E' = &\frac{2}{N-1}\sum_{ab}\sum_{a'b'}\left[\delta_{ab}Q_{aa'}Q_{ab'}\Pi_{ab} + \right. \\ &\left.\left(Q_{aa'}Q_{ab'} + Q_{ba'}Q_{bb'}\right)D_{ab}\right]T_{a'b'} + \\ &\sum_{ab}\sum_{a'b'c'd'} Q_{aa'}Q_{ab'}Q_{bc'}Q_{bd'}V_{a'b'c'd'}\Pi_{ab} + \\ &\sum_{ab}\sum_{a'b'c'd'} Q_{aa'}Q_{bb'}\left(2Q_{ac'}Q_{bd'} - Q_{bc'}Q_{ad'}\right) \\ &V_{a'b'c'd'}D_{ab}\ . \end{aligned} \tag{45}$$

Substituting eq. (44) into eq. (39) yields, after some work, the following expression for the energy,

$$\begin{aligned} E'(\theta)^{kl} = A\cos 4\theta + B\cos 2\theta + C\sin 4\theta \\ + D\sin 2\theta + F \end{aligned} \tag{46}$$

for the rotation over of an angle θ between orbitals k and l. The constants A, B, C, D, F, of which the complete expression is given in the supplementary material[1], depend on the elements of the 2DM, T_{ab} and V_{abcd}. As eq. (46) has a period of π, we only consider the interval $[-\frac{\pi}{2}, \frac{\pi}{2}]$. The N-representability conditions of section 2 are unitarily invariant, so we are guaranteed that a Jacobi rotation does not affect the N-representability, but the energy is not necessarily minimal. This means that the calculated energy (46) will always be greater than or equal to the optimized v2DM minimum.

It is easy and cheap to calculate the gradient and Hessian of this equation. Using a Newton-Raphson algorithm, we can thus easily find the angle for which eq. (46) is minimal. The constant term (F) in eq. (46) is the only one involving a double sum over the orbitals: it is the original double sum appearing in eq. (40) over all orbitals except orbitals k and l. This implies that an evaluation of the energy scales as L^2, but the energy difference, gradient and the Hessian only scale computationally as L. If we iterate over all pairs of orbitals (scaling as L^2) and find the optimal angle for minimization, we have an L^3 algorithm to find the new Jacobi rotation optimizing the energy decrease. If symmetry-adapted orbitals are used, only rotations between orbitals in the same irreducible representation are allowed, which simplifies the two-electron integral transformation even more. A schematic overview is given in Algorithm 1.

Algorithm 1 The algorithm used to find the optimal Jacobi rotation in pseudocode

```
procedure FindOptimalRotation(Γ, T, V)
    for i ← 1, n_irrep do                          ▷ Loop over all irreducible representations
        for all (a, b) ∈ irrep_i do                ▷ Loop over all pairs of orbitals belonging to irrep i
            (E_ab, θ_ab) = FindMinimum(Γ, T, V, a, b)        ▷ Minimum of (46)
        end for
    end for
    (k, l, θ) = min (E, θ)                         ▷ Find the lowest energy over all pairs
    return (k, l, θ_kl)                            ▷ Return the pair of orbitals and the angle
end procedure
```

As an example, we consider the BH molecule at equilibrium distance (2.32 Bohr) in the

[1]See supplemental material at [INSERT URL] for the complete expression of the constants in eq. (46).

STO-3G basis. Figure 3 contains the energy as a function of the rotation angle between several pairs of orbitals starting from the Hartree-Fock molecular orbitals. The full (red) curve is the energy as calculated with eq. (46) keeping the 2DM fixed, whereas the dashed (blue) curve involves a 2DM optimization at each point. We used C_{2v} symmetry for BH (the largest Abelian point group of BH) and we only consider the 4 orbitals that transform according to irreducible representation A_1 (the other 2 orbitals transform according to B_1 and B_2). The orbital energies (in Hartree) of the restricted Hartree-Fock solution are given in Table 2.

Table 2: The restricted Hartree-Fock solution for BH. The orbital energies are in Hartree. We use C_{2v} symmetry, the orbitals are labelled according to irreducible representations A_1, B_1 or B_2.

Doubly occupied orbitals					
$1A_1$	-7.339428	$2A_1$	-0.573370	$3A_1$	-0.246546
Virtual orbitals					
$1B_1$	0.269938	$1B_2$	0.269938	$4A_1$	0.701123

The pictures shown for the BH molecule are characteristic for most calculations that we have done. For most pairs of orbitals, the lowest energy is obtained for very small rotation angles except for a few where a larger decrease in energy can be achieved. In Figure 3b there is a clear new minimum and the angle found using (46) is very close to the v2DM optimized minimum. The $1A_1$ orbital is the localized $1s$ orbital on the Boron atom. The $2A_1$ and $3A_1$ orbitals are a mixture of the $1s$ on the hydrogen atom and the $2s$ and $2p_z$ on the Boron atom. The largest energy gain can be achieved by mixing these orbitals and this already brings us very close to the FullCI energy (-24.810 E_h).

4 Results

We have developed a code to perform variational 2DM optimizations using the DOCI constraints derived in section 2.2 in conjunction with orbital optimization according to eq. (46). The one- and two-particle integrals are transformed with the optimized Jacobi rotation (see

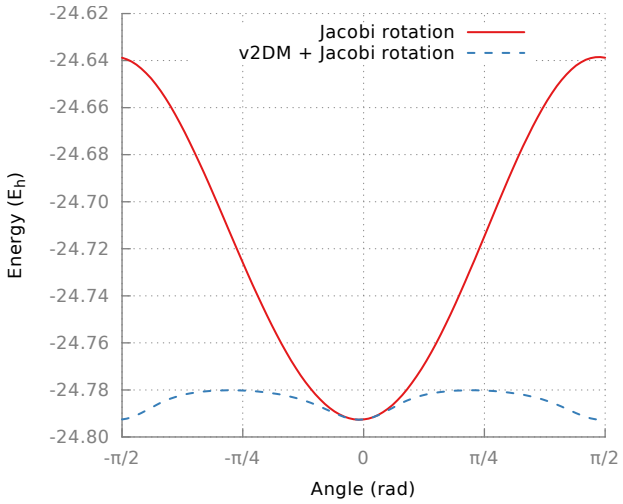

(a) Orbitals $1A_1$ and $2A_1$, min ≈ -0.027 rad

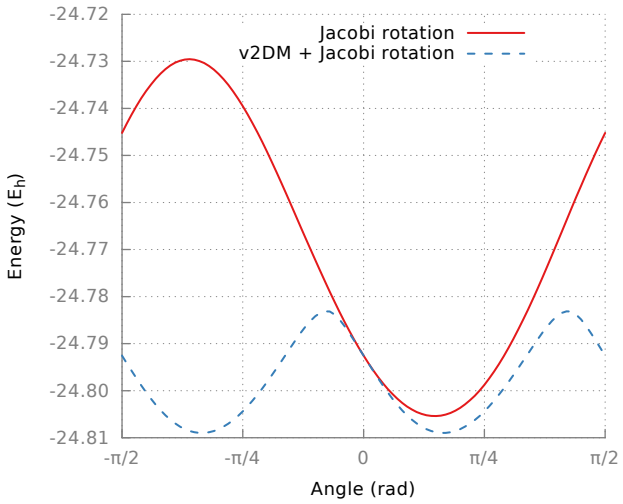

(b) Orbitals $2A_1$ and $3A_1$, min ≈ 0.463 rad

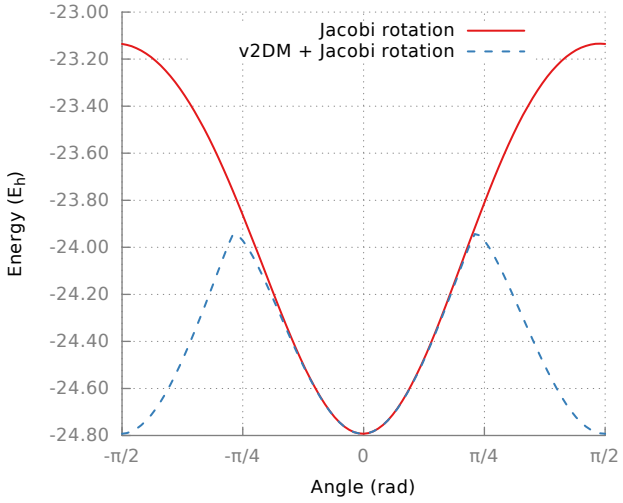

(c) Orbitals $2A_1$ and $4A_1$, min ≈ -0.005 rad

Figure 3: The red curve has been calculated using (46) while the blue curve uses the same transformed reduced Hamiltonian but an optimized 2DM-DOCI. These results are for BH in STO-3G. We used an interatomic distance of 2.32 Bohr. The min refers to the minimum of the eq. (46) (red curve). The FullCI energy is -24.810 E_h.

Algorithm 1) and a new v2DM optimization is started. We continue this loop until the ground-state energy is converged to within 10^{-6} E_h during at least 25 steps. For the v2DM calculations, we used a boundary point method with a primal and dual convergence criterion of 10^{-7} (see ref. 68). The flow of our program is shown in Algorithm 2.

Algorithm 2 Schematic overview of the complete v2DM-DOCI algorithm

converged $\leftarrow 0$
while converged < 25 **do** ▷ Do 25 steps within convergence criteria
  $E_{\text{new}}, \Gamma = \text{v2DM}(T, V)$ ▷ Do a v2DM-DOCI optimization with electron integrals T and V
  $(k, l, \theta) = \text{FindOptimalRotation}(\Gamma, T, V)$ ▷ Find the optimal rotation
  $T, V = \text{TransformIntegrals}(k, l, \theta, T, V)$ ▷ Rotate the integrals
  if $|E_{\text{new}} - E_{\text{old}}| < 10^{-6}$ **then** ▷ Check convergence
    converged $\leftarrow$ converged $+ 1$
  end if
  $E_{\text{old}} \leftarrow E_{\text{new}}$
end while

The code used to generate the data presented can be found online[74] under the GPLv3 license. All simulations were run single-threaded on a Intel Xeon E5-2680 v3 with 64GB of RAM. We used PSI4[75] to generate the one- and two-electron integrals in the Gaussian basis set and the Hartree-Fock molecular orbitals. Unless specified otherwise, the Hartree-Fock molecular orbitals are the starting point for the orbital optimization. In all calculations, the cc-pVDZ basis was used. Benchmark results are provided by CheMPS2[76–79], an open-source spin-adapted implementation of Density Matrix Renormalization Group (DMRG) for ab initio quantum chemistry, that generates results with FullCI accuracy. To monitor the convergence in CheMPS2, we increased the bond dimension in steps from 500 to 2500 for all calculations. FullDOCI is the result of a CI solver restricted to the doubly-occupied Slater determinants, combined with the same orbital optimization scheme as v2DM-DOCI (unless specified otherwise).

4.1 Two- and four-electron systems

The DOCI wavefunction for a two-electron system is exact provided that the orbitals are optimized[15]. General v2DM using only the $\mathcal{P}$ condition is also exact for a two-electron system[30,49]. It is easy to prove that v2DM-DOCI combined with orbital optimization also generates exact results for any two-electron system. This is illustrated by the numerical results in Table 3 for H_2 and He. Note that in Table 3 the FullDOCI results were obtained with the optimal orbitals produced by v2DM-DOCI.

In the dissociated He_2 dimer, the effect of symmetry breaking can be seen in the third and fourth row of Table 3. When we allow the point-group symmetry to break down from D_{2h} to C_1, the orbital optimization algorithm is no longer restricted to orbitals transforming according to the same irreducible representation. When the symmetry is not broken (D_{2h}), the s orbitals of the two He atoms are coupled, in the sense that only (anti-)symmetric combinations are retained. In this case v2DM-DOCI cannot recover the FullCI energy. When we decouple the orbitals and use C_1 symmetry, the full correlation energy is found. It is important to note the difference with the general v2DM optimization: general v2DM always gives a lower bound to the exact ground-state energy, but in the v2DM-DOCI case, the energy is orbital dependent. The v2DM-DOCI energy can be higher or lower than the FullCI result. We almost always find a higher energy. It is still true, however, that the v2DM-DOCI must be lower than or equal to FullDOCI with the same set of orbitals. In principle we combine a lower-bound method (v2DM) with an upper-bound method (Jacobi

Table 3: Ground-state energy for some small systems in the cc-pVDZ basis. Energies are in milliHartree, interatomic distance (d) in Bohr. The columns labeled v2DM-DOCI and FullDOCI contain the deviation from FullCI. The orbital optimization is done with the specified Abelian symmetry in the column labeled 'Sym.'

System	Sym.	d	HF	FullCI	Δv2DM-DOCI	ΔFullDOCI
H_2	D_{2h}	1.438	-1128.629	-1163.673	0.000	0.000
He	D_{2h}		-2855.160	-2887.595	0.000	0.000
He_2	D_{2h}	10.000	-5710.321	-5775.190	40.013	40.022
He_2	C_1	10.000	-5710.321	-5775.190	0.000	0.000

rotations). A cancelation of errors can occur and that is why we always compare to FullDOCI as it uses an exact energy solver.

4.2 Hydrogen chain

The symmetric stretching of an equidistant chain of hydrogen atoms is a standard test case for a new method aimed at strong static correlations. It is simple yet challenging, because of the strong correlation effects in the transition from metallic hydrogen to dissociated hydrogen. We use a H_8 chain[15,19] in the cc-pVDZ basis with D_{2h} (symmetry-adapted) or C_1 (symmetry-broken) orbitals. The results shown in Figure 4 indicate the importance of the choice of the starting point in the orbital optimization scheme as this dictates the valley in which the local minimizer is active. The underlying basis for the one- and two-electron integrals is always

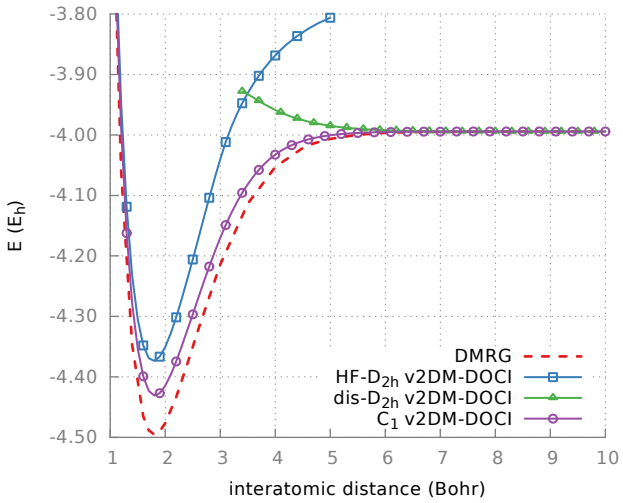

Figure 4: The symmetric stretch of H_8 in the cc-pVDZ basis. Not all calculated points are marked. For the C_1 curve, the largest deviation from DMRG is 45 milliHartree around the minimum at 1.8 Bohr.

taken to be the Löwdin orthogonalized Gaussian basis set (symmetry-adapted if specified). For the HF-D_{2h} curve, we first performed a calculation at equilibrium distance starting from the Hartree-Fock molecular orbitals. The resulting orthogonal transformation matrix, describing the transition from the Löwdin orthogonalized Gaussian basis set to the optimal set of orbitals at equilibrium, was used as a starting point in the orbital optimization for all

other points on the curve. It is clear from the figure that this procedure does not lead to a satisfactory description of the metallic to the non-interacting region, as the dissociation limit is much higher in energy than the FullCI curve.

For the curve labeled dis-D_{2h}, we performed a calculation at 10 Bohr determining the optimal orbital transformation with a random search and used this orbital transformation as a starting point for all other distances in the curve. This procedure correctly describes the dissociation limit but the energy rises artificially when we go into the metallic regime. So symmetry-adapted D_{2h} orbitals cannot describe the transition from metallic to non-interacting, localized hydrogen atoms. When starting from several random points, we could not find a lower energy curve for the D_{2h} case. The whole picture changes when we break the symmetry (the curve labeled C_1), and v2DM-DOCI now gives a physically correct description of the transition. This curve was found by starting from the optimal orbital transformation of a v2DM-DOCI calculation at 10 Bohr using localized orbitals as starting point. Similar results were already reported by Bytautas et al.[15]: they verified that the behaviour is not a two-state crossing or avoided crossing between the ground state and an excited state.

In Figure 5, we have plotted the natural orbital occupation numbers from the 1DM extracted from v2DM-DOCI, for both symmetries. In the C_1 symmetry there is a smooth transition from doubly-occupied hydrogen to singly-occupied hydrogen. In the D_{2h} symmetry the 'localized' orbitals corresponding to dis-D_{2h} curve in Figure 4 have a branch of singly-occupied hydrogen that is not present in the C_1 symmetry. The 'molecular orbitals' corresponding to the HF-D_{2h} curve in Figure 4 also have branches with no counterpart in the localized orbitals. It is clear that only v2DM-DOCI results with symmetry-broken optimized orbitals provide a correct description of the transition.

As far as the details of the orbital optimization scheme are concerned, we found that the procedure can be accelerated by not performing a v2DM-DOCI optimization at each rotation: in practice we see that the energy decreases considerably in the first steps. In subsequent steps, the convergence goes more slowly as the algorithm can only update two

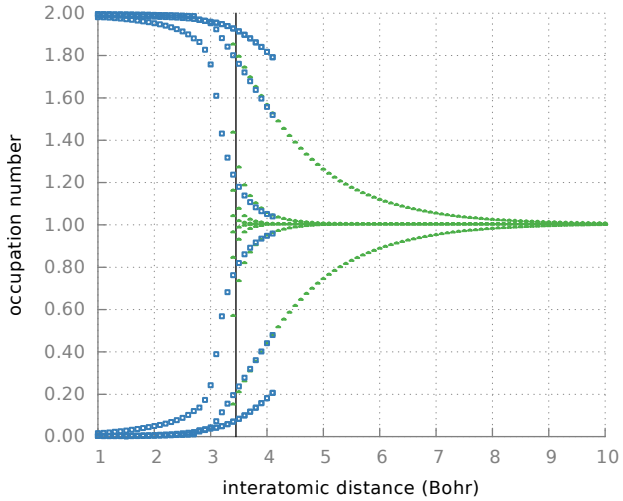

(a) The natural occupation numbers of H_8 for the D_{2h} symmetry

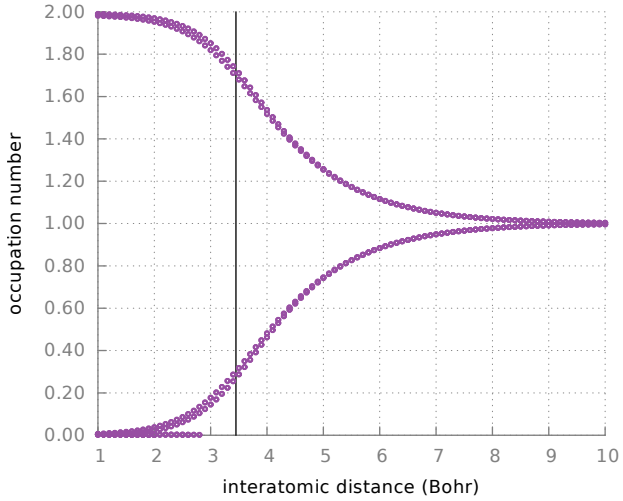

(b) The natural occupation numbers of H_8 for the C_1 symmetry

Figure 5: The v2DM-DOCI natural orbital occupation numbers for both symmetries of the symmetric stretch of H_8. Only points with an occupation number larger than 10^{-3} are shown. The black line marks the energy crossing of the D_{2h} curves in Figure 4. The colors also match the curves in Figure 4.

orbitals at a time. In this tail of the minimization, we can safely skip the optimization of the 2DM for a number of updates as all rotation angles are small, only to restart the algorithm with the optimal solution from the previous step at the very end. This technique partially circumvents the downside of the Jacobi rotations, i.e. that only two orbitals are updated at the same time.

4.3 Molecular systems

Another interesting test is the dissociation of a diatomic molecule in which static correlation is of paramount importance at dissociation. The cc-pVDZ basis is used for all molecules. The nomenclature used for the results is as follows: v2DM-DOCI refers to v2DM with the DOCI constraints on the 2DM (see section 2.2) and with the Jacobi orbital optimization (see section 3). FullDOCI uses the same orbital optimization algorithm. v2DM-DOCI/FullDOCI is a single-shot v2DM-DOCI calculation using the optimal set of orbitals from a FullDOCI calculation. FullDOCI/v2DM-DOCI is exactly the opposite: a single-shot FullDOCI calculation using the optimal set of orbitals from v2DM-DOCI.

We first present the dissociation of N_2. This is challenging because of the breaking of a triple bond and is often used as a test case[15,80–83]. In the cc-pVDZ basis, N_2 has 28 orbitals and we perform calculations with both D_{2h} and C_1 symmetry. The results are presented in Figure 6 and detailed in Table 4. The results are to be compared to DMRG calculations[76–79] which are to be considered as the FullCI reference. In order to appreciate the performance of v2DM-DOCI, results of other methods such as Coupled-Cluster with Singles, Doubles and perturbative Triples (CCSD(T))[84] and density functional theory with B3LYP functional[85,86] are also presented. All DOCI curves give a qualitatively correct description of the dissociation process. In Table 4 one can notice that v2DM-DOCI is a better approximation to FullDOCI than v2DM is to FullCI. The effect of symmetry breaking is very small for N_2: the energy gains are in the milliHartree region. Note that N_2 dissociates into two N atoms with an odd number of electrons. This forms no problem for FullDOCI as the orbital optimization can

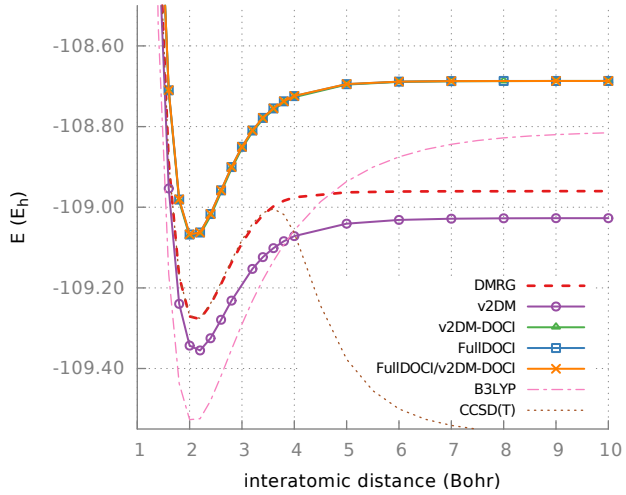

Figure 6: The dissociation of N_2 in the cc-pVDZ basis. The DOCI curves shown are for the C_1 symmetry. Note that three curves (v2DM-DOCI, FullDOCI, FullDOCI/v2DM-DOCI) coincide visually.

Table 4: Some points on the N_2 curve from Figure 6. The interatomic distance (d) is in Bohr. The DMRG energy is in Hartree. For v2DM, v2DM-DOCI and FullDOCI, the deviation from DMRG is given in milliHartree.

d	Sym.	DMRG	Δv2DM	Δv2DM-DOCI	ΔFullDOCI
2.2	D_{2h}	-109.278	-77.375	222.578	224.455
2.2	C_1	-109.278	-77.375	209.891	214.787
4.0	D_{2h}	-108.975	-96.213	257.013	258.842
4.0	C_1	-108.975	-96.213	248.396	250.991
10.0	D_{2h}	-108.960	-66.384	282.966	283.108
10.0	C_1	-108.960	-66.384	273.371	273.464

handle this[24]. The difference between the DOCI curves and the DMRG reference is due to dynamical correlations and can be added in a subsequent stage, as shown in Ref. 87.

Another interesting case is cyanide, CN^-. This heteronuclear molecule also has a triple bond and dissociates in C^- and N. The effect of breaking the C_{2v} symmetry is again minimal (see results in Table 5) so in Figure 7 we restrict ourself to the C_1 curve. For this het-

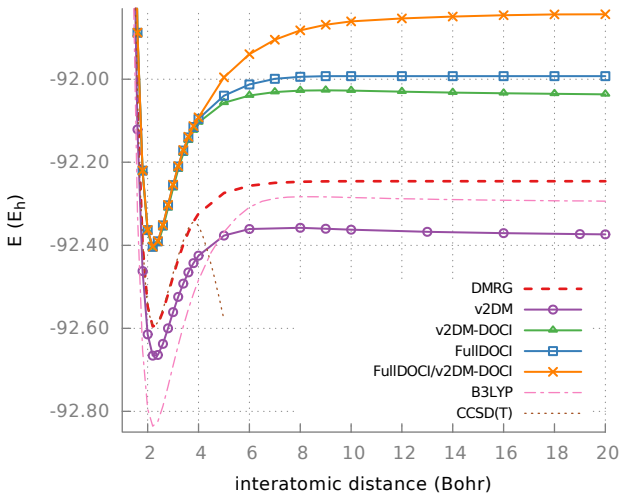

Figure 7: The dissociation of CN^- in the cc-PVDZ basis. The DOCI curves shown are for the C_1 symmetry.

Table 5: Some points on the CN^- curve from Figure 7. The interatomic distance (d) is in Bohr. The DMRG energy is in Hartree. For v2DM, v2DM-DOCI and FullDOCI, the deviation from DMRG is given in milliHartree.

d	Sym.	DMRG	Δv2DM	Δv2DM-DOCI	ΔFullDOCI
2.2	C_{2v}	-92.596	-70.208	186.967	192.202
2.2	C_1	-92.596	-70.208	186.967	192.192
4.0	C_{2v}	-92.324	-101.281	219.639	228.307
4.0	C_1	-92.324	-101.281	219.639	228.300
10.0	C_{2v}	-92.246	-116.686	218.333	253.131
10.0	C_1	-92.246	-116.686	218.333	253.130
20.0	C_{2v}	-92.246	-127.996	209.275	253.135
20.0	C_1	-92.246	-127.996	209.275	253.133

eronuclear molecule, the dissociation limit for v2DM and v2DM-DOCI is incorrect. This is a known failure for v2DM-based techniques[88]: the energy of the isolated atoms as a function of fractional charge is a convex curve in v2DM whereas it should be a piecewise linear curve[89].

Because of this, v2DM will favour fractional charges on dissociated atoms and thus give a physically incorrect picture. This can be seen clearly on the FullDOCI/v2DM-DOCI curve: if we use the optimal basis of v2DM-DOCI, the FullDOCI energy is much higher than the true FullDOCI energy as the FullDOCI solution cannot use the artificial non-integer atomic charges. A Mulliken population analysis[90] confirms this: at an interatomic distance of 20 Bohr, the net charges are $C^{-0.48}N^{-0.52}$. Using so-called subsystem constraints[34,91] one can force the E vs N curve to be piecewise linear. However, this would require a v2DM(-DOCI) optimization at each nearby integer value of N. In Figure 8, we have used the FullDOCI optimal orbitals for the v2DM-DOCI calculation. In this case, v2DM-DOCI gives the correct DOCI dissociation limit. This suggests that it might be possible to find specific DOCI constraints to solve the problem of fractional charges in v2DM-DOCI.

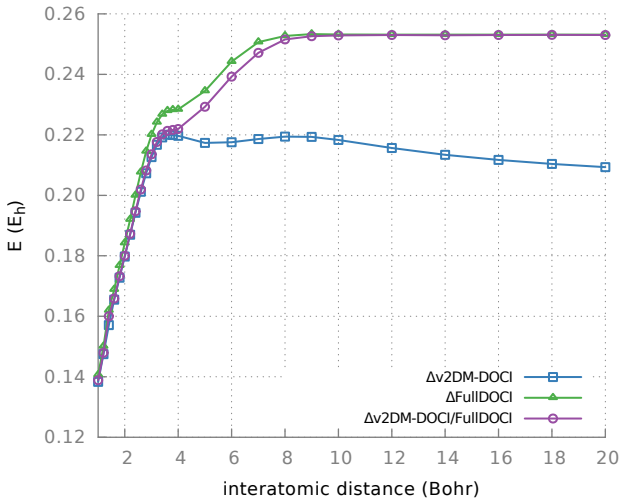

Figure 8: The dissociation of CN^- in the cc-PVDZ basis: comparing the v2DM-DOCI/FullDOCI results with v2DM-DOCI and FullDOCI. The deviation from DMRG is plotted.

5 Conclusion

In this paper we applied specific necessary N-representability constraints for a second order density matrix derived from a seniority-zero CI wavefunction. The standard two-particle

conditions $\mathcal{P}$, $\mathcal{Q}$ and $\mathcal{G}$ reduce to a simpler form that allows for a better theoretical scaling: L^3 instead of L^6. As any truncated CI wavefunction is orbital dependent, an orbital optimization scheme has been included. We use an orbital optimizer based on elementary Jacobi rotations. Only two orbitals are optimized at each step, implying that the associated two-electron integral transformation is much more efficient. The theoretical scaling of the orbital optimizer is L^3. In practice, the molecular systems in this manuscript needed less than 50 Jacobi rotations with optimization to convergence. The runtime was on average less than one hour. Both of course are very dependent on the used starting point. We have tested our method on several challenging cases. For the H_8 equidistant chain, we find that the symmetry of the system must be broken in order to find the correct DOCI energy curve. The orbital optimizer needs the additional degrees of freedom to find the physically correct set of orbitals. For the dissociation of N_2, v2DM-DOCI gives good results, and symmetry breaking hardly gives any improvement. It is seen that v2DM-DOCI provides a good approximation to FullDOCI: the v2DM-DOCI and FullDOCI energies are consistently closer to each other than the v2DM and FullCI energies. In the dissociation of CN^-, v2DM and v2DM-DOCI fail due to fractional charges although FullDOCI still gives a good description. We note that v2DM-DOCI with the FullDOCI optimal basis can reproduce the correct FullDOCI energy. This indicates that there could exist specific DOCI constraints to fix the problem of fractional charges in v2DM-DOCI.

The orbital optimizer works well provided it is given a suitable starting point. Near equilibrium, the Hartree-Fock molecular orbitals are usually a good choice, whereas in the dissociation limit localized orbitals often give a better starting point. Unfortunately this does not always hold: for instance for the H_8 chain the equilibrium energy could only be found by starting from the localized orbitals. However, if a single optimal point is found in the correct DOCI valley, it can usually be used as a starting point for all other calculations on the same system.

The main results of this paper support the idea that DOCI combined with orbital op-

timization captures the lion's share of the static correlations. Subsequently, the missing dynamic correlations can be added through perturbation theory. We find that v2DM-DOCI is a good and fast approximation to FullDOCI.

Acknowledgement

W.P., M.V.R., B.V., S.D.B., P.B. and D.V.N. are members of the QCMM alliance Ghent-Brussels. W.P., S.D.B. and B.V. acknowledge the support from the Research Foundation Flanders (FWO Vlaanderen). P.B. and D.R.A. acknowledge the Research Foundation Flanders (FWO Vlaanderen) and the Ministerio de Ciencia, Tecnología e Innovación Productiva (Argentina) for a collaborative research grant. A.T. and L.L. acknowledge the Universidad del Pais Vasco (Spain) for the research grants No. GIU12/09 and UFI11/07. D.R.A. acknowledges the Universidad de Buenos Aires (Argentina) and the Consejo Nacional de Investigaciones Científicas y Técnicas (Argentina) for the research grants No. UBACYT 20020100100197, PIP 11220090100061 and PIP 11220130100377CO. The computational resources (Stevin Supercomputer Infrastructure) and services used in this work were provided by the VSC (Flemish Supercomputer Center), funded by Ghent University, the Hercules Foundation and the Flemish Government - department EWI. W.P. would like to thank Paul Ayers and Pieter Claeys for the fruitful discussions.

Supporting Information Available

In the supporting information a complete expression of eq. (46) including the constants A, B, C, D, F can be found. This material is available free of charge via the Internet at `http://pubs.acs.org/`.

References

(1) Helgaker, T.; Jorgensen, P.; Olsen, J. *Molecular Electronic-Structure Theory*; Wiley: New York, 2014; pp 142–201.

(2) Szabo, A.; Ostlund, N. S. *Modern Quantum Chemistry: Introduction to Advanced Electronic Structure Theory*; Dover Publications: New York, 1996; pp 108–271.

(3) Crawford, T. D.; Schaefer, H. F. *Reviews in Computational Chemistry*; Wiley: New York, 2007; pp 33–136.

(4) Bartlett, R. J.; Musiał, M. *Rev. Mod. Phys.* **2007**, *79*, 291–352.

(5) David, S. C.; Antara, D.; L., A. M.; S., S. J. *Electron Correlation Methodology*; Chapter 6, pp 75–88.

(6) Szalay, P. G.; Müller, T.; Gidofalvi, G.; Lischka, H.; Shepard, R. *Chem. Rev.* **2012**, *112*, 108–181.

(7) White, S. R. *Phys. Rev. Lett.* **1992**, *69*, 2863–2866.

(8) White, S. R.; Martin, R. L. *J. Chem. Phys.* **1999**, *110*, 4127–4130.

(9) Chan, G. K.-L.; Head-Gordon, M. *J. Chem. Phys.* **2002**, *116*, 4462–4476.

(10) Schollwöck, U. *Ann. Phys.* **2011**, *326*, 96 – 192, January 2011 Special Issue.

(11) Fukutome, H. *Int. J. Quantum Chem.* **1981**, *20*, 955–1065.

(12) Stuber, J. L.; Paldus, J. In *Symmetry breaking in the independent particle model*; Brändas, E. J., Kryachko, E. S., Eds.; Fundamental World of Quantum Chemistry, A Tribute Volume to the Memory of Per-Olov Löwdin; Kluwer Academic: Dordrecht, The Nederlands, 2003; Vol. 1; Chapter 4, pp 67–139.

(13) Jiménez-Hoyos, C. A.; Henderson, T. M.; Scuseria, G. E. *J. Chem. Theory Comput.* **2011**, *7*, 2667–2674.

(14) Jiménez-Hoyos, C. A.; Henderson, T. M.; Tsuchimochi, T.; Scuseria, G. E. *J. Chem. Phys.* **2012**, *136*, 164109.

(15) Bytautas, L.; Henderson, T. M.; Jiménez-Hoyos, C. A.; Ellis, J. K.; Scuseria, G. E. *J. Chem. Phys.* **2011**, *135*, 044119.

(16) Boguslawski, K.; Tecmer, P.; Ayers, P. W.; Bultinck, P.; De Baerdemacker, S.; Van Neck, D. *Phys. Rev. B* **2014**, *89*, 201106.

(17) Stein, T.; Henderson, T. M.; Scuseria, G. E. *J. Chem. Phys.* **2014**, *140*, 214113.

(18) Johnson, P. A.; Ayers, P. W.; Limacher, P. A.; De Baerdemacker, S.; Van Neck, D.; Bultinck, P. *Comput. Theor. Chem.* **2013**, *1003*, 101–113.

(19) Limacher, P. A.; Ayers, P. W.; Johnson, P. A.; De Baerdemacker, S.; Van Neck, D.; Bultinck, P. *J. Chem. Theory Comput.* **2013**, *9*, 1394–1401.

(20) Henderson, T. M.; Bulik, I. W.; Stein, T.; Scuseria, G. E. *J. Chem. Phys.* **2014**, *141*, 244104.

(21) Ring, P.; Schuck, P. *The Nuclear Many-Body Problem*; Springer-Verlag: Berlin, 2005; pp 221–228.

(22) Alcoba, D. R.; Torre, A.; Lain, L.; Massaccesi, G. E.; Oña, O. B. *J. Chem. Phys.* **2013**, *139*, 084103.

(23) Alcoba, D. R.; Torre, A.; Lain, L.; Oña, O. B.; Capuzzi, P.; Van Raemdonck, M.; Bultinck, P.; Van Neck, D. *J. Chem. Phys.* **2014**, *141*, 244118.

(24) Limacher, P. A.; Kim, T. D.; Ayers, P. W.; Johnson, P. A.; De Baerdemacker, S.; Van Neck, D.; Bultinck, P. *Mol. Phys.* **2014**, *112*, 853–862.

(25) Alcoba, D. R.; Torre, A.; Lain, L.; Massaccesi, G. E.; Oña, O. B. *J. Chem. Phys.* **2014**, *140*, 234103.

(26) Husimi, K. *Proc. Phys.-Math. Soc. Japan* **1940**, *22*, 264.

(27) Löwdin, P.-O. *Phys. Rev.* **1955**, *97*, 1474–1489.

(28) Mayer, J. *Phys. Rev.* **1955**, *100*, 6.

(29) Tredgold, R. H. *Phys. Rev.* **1957**, *105*, 5.

(30) Coleman, A. J. *Rev. Mod. Phys.* **1963**, *35*, 668–686.

(31) Liu, Y.-K.; Christandl, M.; Verstraete, F. *Phys. Rev. Lett.* **2007**, *98*, 110503.

(32) Garrod, C.; Percus, J. K. *J. Math. Phys.* **1964**, *5*, 1756–1776.

(33) Zhao, Z.; Braams, B. J.; Fukuda, M.; Overton, M. L.; Percus, J. K. *J. Chem. Phys.* **2004**, *120*, 5.

(34) Verstichel, B.; van Aggelen, H.; Van Neck, D.; Ayers, P. W.; Bultinck, P. *J. Chem. Phys.* **2010**, *132*, 114113.

(35) Shenvi, N.; Izmaylov, A. F. *Phys. Rev. Lett.* **2010**, *105*, 213003.

(36) Vandenberghe, L.; Boyd, S. *SIAM Rev.* **1996**, *38*, 49–95.

(37) Nesterov, Y. E.; Todd, M. J. *Math. Oper. Res.* **1997**, *22*, 1–42.

(38) Nesterov, Y.; Nemirovski, A. *Interior Point Polynomial Algorithms in Convex Programming*; Studies in Applied and Numerical Mathematics; SIAM: Philadelphia, 1994; Vol. 13; pp 57–147.

(39) Yamashita, M.; Fujisawa, K.; Fukuda, M.; Kobayashi, K.; Nakata, K.; Nakata, M. In *Handbook on Semidefinite, Conic and Polynomial Optimization*; Anjos, M. F.,

Lasserre, J. B., Eds.; International Series in Operations Research & Management Science; Springer US, 2012; Vol. 166; pp 687–713.

(40) Verstichel, B.; van Aggelen, H.; Poelmans, W.; Wouters, S.; Van Neck, D. *Comput. Theor. Chem.* **2013**, *1003*, 12–21.

(41) Mazziotti, D. A. *Phys. Rev. Lett.* **2011**, *106*, 083001.

(42) Mazziotti, D. A. *Phys. Rev. Lett.* **2004**, *93*, 213001.

(43) Verstichel, B.; van Aggelen, H.; Van Neck, D.; Bultinck, P.; De Baerdemacker, S. *Comput. Phys. Commun.* **2011**, *182*, 1235–1244.

(44) Verstichel, B.; van Aggelen, H.; Van Neck, D.; Ayers, P. W.; Bultinck, P. *Comput. Phys. Commun.* **2011**, *182*, 2025–2028.

(45) Mazziotti, D. A. *Acc. Chem. Res.* **2006**, *39*, 207–215.

(46) Nakata, M.; Nakatsuji, H.; Ehara, M.; Fukuda, M.; Nakata, K.; Fujisawa, K. *J. Chem. Phys.* **2001**, *114*, 19.

(47) Mazziotti, D. A. *Phys. Rev. A* **2002**, *65*, 062511.

(48) Nakata, M.; Braams, B. J.; Fujisawa, K.; Fukuda, M.; Percus, J. K.; Yamashita, M.; Zhao, Z. *J. Chem. Phys.* **2008**, *128*, 164113.

(49) Verstichel, B.; van Aggelen, H.; Van Neck, D.; Ayers, P. W.; Bultinck, P. *Phys. Rev. A* **2009**, *80*, 032508.

(50) van Aggelen, H.; Verstichel, B.; Bultinck, P.; Van Neck, D.; Ayers, P. W.; Cooper, D. L. *J. Chem. Phys.* **2010**, *132*, 114112.

(51) Weinhold, F.; Wilson, E. B. *J. Chem. Phys.* **1967**, *46*, 2752–2758.

(52) Weinhold, F.; Wilson, E. B. *J. Chem. Phys.* **1967**, *47*, 2298–2311.

(53) Siegbahn, P.; Heiberg, A.; Roos, B.; Levy, B. *Phys. Scr.* **1980**, *21*, 323.

(54) Ruedenberg, K.; Cheung, L. M.; Elbert, S. T. *Int. J. Quantum Chem.* **1979**, *16*, 1069–1101.

(55) Rashid, Z.; Lenthe, J. H. v. *J. Chem. Phys.* **2013**, *138*, 054105.

(56) Roos, B. O.; Taylor, P. R.; Siegbahn, P. E. *Chem. Phys.* **1980**, *48*, 157 – 173.

(57) Lengsfield, B. H. *J. Chem. Phys.* **1980**, *73*, 382–390.

(58) Raffenetti, R.; Ruedenberg, K.; Janssen, C.; Schaefer, H. *Theor. Chim. Acta* **1993**, *86*, 149–165.

(59) Dickhoff, W. H.; Van Neck, D. *Many-Body Theory Exposed!*; World Scientific: Singapore, 2008; pp 17–31.

(60) Ayers, P. W. *Phys. Rev. A* **2006**, *74*, 042502.

(61) Van Neck, D.; Ayers, P. W. *Phys. Rev. A* **2007**, *75*, 032502.

(62) Hammond, J. R.; Mazziotti, D. A. *Phys. Rev. A* **2005**, *71*, 062503.

(63) Mazziotti, D. A. *Phys. Rev. A* **2006**, *74*, 032501.

(64) Mazziotti, D. A. *Reduced-Density-Matrix Mechanics: With Application to Many-Electron Atoms and Molecules*; Wiley: New York, 2007; pp 19–59.

(65) Braams, B. J.; Percus, J. K.; Zhao, Z. *Reduced-Density-Matrix Mechanics: With Application to Many-Electron Atoms and Molecules*; Wiley: New York, 2007; pp 93–101.

(66) Yamashita, M.; Fujisawa, K.; Kojima, M. *Optim. Method. Softw.* **2003**, *18*, 491–505.

(67) SDPA (SemiDefinite Programming Algorithm). `http://sdpa.sourceforge.net`, (accessed April 20, 2015).

(68) Verstichel, B. Variational determination of the two-particle density matrix as a quantum many-body technique. Ph.D. thesis, Ghent University, 2012.

(69) Povh, J.; Rendl, F.; Wiegele, A. *Computing* **2006**, *78*, 277–286.

(70) Malick, J.; Povh, J.; Rendl, F.; Wiegele, A. *SIAM J. Optim.* **2009**, *20*, 336–356.

(71) Olsen, J.; Yeager, D. L.; Jørgensen, P. *Advances in Chemical Physics*; Wiley: New York, 2007; pp 1–176.

(72) Schmidt, M. W.; Gordon, M. S. *Annu. Rev. Phys. Chem.* **1998**, *49*, 233–266.

(73) Lengsfield, B. H.; Liu, B. *J. Chem. Phys.* **1981**, *75*, 478–480.

(74) Poelmans, W. v2DM-DOCI solver. `https://github.com/wpoely86/doci_sdp-atom`, (accessed May 3, 2015).

(75) Turney, J. M.; Simmonett, A. C.; Parrish, R. M.; Hohenstein, E. G.; Evangelista, F. A.; Fermann, J. T.; Mintz, B. J.; Burns, L. A.; Wilke, J. J.; Abrams, M. L.; Russ, N. J.; Leininger, M. L.; Janssen, C. L.; Seidl, E. T.; Allen, W. D.; Schaefer, H. F.; King, R. A.; Valeev, E. F.; Sherrill, C. D.; Crawford, T. D. *WIREs Comput Mol Sci* **2012**, *2*, 556–565.

(76) Wouters, S.; Poelmans, W.; Ayers, P. W.; Neck, D. V. *Comput. Phys. Commun.* **2014**, *185*, 1501 – 1514.

(77) Wouters, S.; Poelmans, W.; Baerdemacker, S. D.; Ayers, P. W.; Neck, D. V. *Comput. Phys. Commun.* **2015**, *191*, 235 – 237.

(78) Wouters, S.; Van Neck, D. *Eur. Phys. J. D* **2014**, *68*.

(79) Wouters, S.; Bogaerts, T.; Van Der Voort, P.; Van Speybroeck, V.; Van Neck, D. *J. Chem. Phys.* **2014**, *140*, 241103.

(80) Kats, D.; Manby, F. R. *J. Chem. Phys.* **2013**, *139*, 021102.

(81) Li, X.; Paldus, J. *J. Chem. Phys.* **2000**, *113*, 9966–9977.

(82) Couty, M.; Hall, M. B. *J. Phys. Chem. A* **1997**, *101*, 6936–6944.

(83) Chan, G. K.-L.; Kállay, M.; Gauss, J. *J. Chem. Phys.* **2004**, *121*, 6110–6116.

(84) Raghavachari, K.; Trucks, G. W.; Pople, J. A.; Head-Gordon, M. *Chem. Phys. Lett.* **1989**, *157*, 479 – 483.

(85) Becke, A. D. *J. Chem. Phys.* **1993**, *98*, 1372–1377.

(86) Lee, C.; Yang, W.; Parr, R. G. *Phys. Rev. B* **1988**, *37*, 785–789.

(87) Limacher, P. A.; Ayers, P. W.; Johnson, P. A.; De Baerdemacker, S.; Neck, D. V.; Bultinck, P. *Phys. Chem. Chem. Phys.* **2014**, *16*, 5061–5065.

(88) Van Aggelen, H.; Bultinck, P.; Verstichel, B.; Van Neck, D.; Ayers, P. W. *Phys. Chem. Chem. Phys.* **2009**, *11*, 5558–5560.

(89) Yang, W.; Zhang, Y.; Ayers, P. W. *Phys. Rev. Lett.* **2000**, *84*, 5172–5175.

(90) Mulliken, R. S. *J. Chem. Phys.* **1955**, *23*, 1833–1840.

(91) van Aggelen, H.; Verstichel, B.; Bultinck, P.; Neck, D. V.; Ayers, P. W.; Cooper, D. L. *J. Chem. Phys.* **2011**, *134*, 054115.